Acta Cryst. (1990). B46, 795–806

Temperature Dependence of Thermal Motion in Crystalline Anthracene

BY CAROLYN PRATT BROCK

Department of Chemistry, University of Kentucky, Lexington, KY 40506-0055, *USA*

AND JACK D. DUNITZ

Organic Chemistry Laboratory, Swiss Federal Institute of Technology, ETH-Zentrum, CH-8092 *Zürich, Switzerland*

(*Received* 14 *March* 1990; *accepted* 13 *July* 1990)

Abstract

Single-crystal X-ray diffraction data for anthracene, $C_{14}H_{10}$, have been measured at six temperatures from 94 to 295 K. Positional and displacement parameters for C and H atoms were refined at each temperature by conventional least-squares techniques. The derived anisotropic displacement parameters for the C atoms at each of the six temperatures were corrected for the contributions of the internal modes and were then analyzed to determine translational (**T**) and librational (**L**) tensors describing the rigid-body molecular motion. Although the resulting **T** and **L** tensors agree well with those measured and calculated previously at room temperature, the shrinkage of the **L** tensor with crystal cooling appears somewhat anomalous. The unexpected behavior is concentrated in the component of **L** associated with the long molecular axis, a component that is, as a consequence of the molecular geometry, relatively poorly determined. Therefore, while the possibility of some subtle, temperature-dependent structural change, such as a molecular reorientation, cannot be ruled out, neither can it be endorsed. This study underlines how the geometry of the molecule being studied can limit the quality of the rigid-body thermal-motion description determined by diffraction methods.

Introduction

The crystal structure of anthracene was first determined by Robertson (1933), and has been studied many times since. New photographic data were collected (Mathieson, Robertson & Sinclair, 1950) and were used for structure refinements by Sinclair, Robertson & Mathieson (1950), Cruickshank (1956*a*, 1957) and Sparks (1958); Sparks also used unpublished counter data collected by D. C. Phillips. Cruickshank & Sparks (1960) reviewed these early studies. Multiple-temperature work on anthracene was initiated by Mason (1964) with new photographic data at 95 and 290 K. Cell constants were measured at nine temperatures between 78 and 440 K by Ryzhenkov, Kozhin & Myasnikova (1969), and structure analyses at 100 and 300 K were reported by Ponomarev & Shilov (1983). Neutron diffraction studies of perdeuteroanthracene were carried out at 298 K (Lehmann & Pawley, 1972) and 16 K (Chaplot, Lehner & Pawley, 1982). One might well ask whether there is still anything about the anthracene structure left to be discovered by standard diffraction techniques.

The present study was initiated in 1981 in parallel with a study of the temperature dependence of the anisotropic displacement parameters (ADP's) in crystalline naphthalene (Brock & Dunitz, 1982). We aimed to determine whether the components of the molecular translational (**T**) and librational (**L**) tensors decreased in the predicted manner (Cruickshank, 1956*b*) as the temperature was lowered. Naphthalene and anthracene crystals were chosen for study because they are paradigms of the molecular solid state and had been investigated by numerous techniques. The results for naphthalene were very satisfactory, but those for anthracene were somewhat perplexing. While the diagonal components of the **T** tensor and of two of the components of the **L** tensor followed the expected kind of temperature dependence, the third component of **L** behaved anomalously. The component that behaves anomalously, hereafter $L^{11}_{\rm int}$, is associated with the longest molecular axis, that is, the axis with the smallest moment of inertia. At the time the anthracene data were measured and first analyzed, there was considerable discussion about the putative existence of a second, triclinic, phase of anthracene that was supposed to be induced by shear forces (Ramdas, Parkinson, Thomas, Gramaccioli, Filippini, Simonetta & Goringe, 1980). It therefore seemed possible that our study had been complicated by an incomplete phase transition driven by the crystal strain resulting from thermal contraction.

We have not published the anthracene study until now because we were unsure of the significance of the

0108-7681/90/060795-12$03.00

unusual behavior of the component L^{11}_{int}. Few other mulitple-temperature studies of molecular crystals were available for comparison. Despite the uncertainties we think the results of this study are provocative: either the anomalous behavior is real and demands explanation, or our data (which we consider to be of above average quality) are insufficient for a definitive determination of the temperature dependence of the molecular motion.

Data collection

Crystals of anthracene were cut from large flat plates grown from butyl acetate or 1-amyl acetate. Four crystals were examined in some detail. Each was attached to a glass fiber with epoxy resin and coated with a thin layer of the adhesive in an attempt to prevent shattering as the temperature was lowered. The same strategy had proved successful during the study of naphthalene (Brock & Dunitz, 1982). Crystals were mounted on an Enraf–Nonius CAD-4/F diffractometer using Mo $K\alpha$ radiation (graphite monochromator, $\lambda = 0{\cdot}71073$ Å) and equipped with a locally modified LT-1 low-temperature attachment.

The widths of the diffraction peaks of all four crystals increased by a factor of 1·5 to 2·0 as the temperature was lowered from 295 to *ca* 95 K. The parameter WIDTH (=RSCANG/3) of the CAD-4 operating system measures the approximate width of the peak at its base. The average values of WIDTH for the four anthracene crystals examined increased from *ca* 0·20° at 295 K to 0·36–0·41° at *ca* 95 K (θ values in the range 10–19°; the $K\alpha_1 - K\alpha_2$ splitting contributes 0·06–0·13° to WIDTH in this range). The WIDTH value at 295 K is typical of a good molecular crystal, and the increase in WIDTH with decreasing temperature is not abnormal.

The first two crystals were cooled at a rate of 40–50 K h^{-1}. The first was abandoned because of the twofold increase in peak width at 95 K; the second was lost overnight, presumably as a result of shattering. The behavior of the third crystal, which was also cooled at 40–50 K h^{-1}, was similar to that of the first. We decided, however, to collect data for this quite large (0·50 × 0·50 × 0·15 mm) crystal at 94 K because it seemed unlikely that a better crystal would be found. A good orientation matrix was obtained, but after *ca* 10 h at 94 K, just as data collection began, the crystal moved appreciably and the peaks became noticeably broader and more asymmetric. The deviations between the observed and calculated peak positions could not be reduced to their previous levels. Data collection at 94 K was continued, but after it was completed, study of the third crystal was abandoned. Microscopic examination of the crystal revealed the development of several prominent fault planes. Results of the refinements of data for this crystal are included, however, to allow comparisons of geometric and thermal parameters determined for two different samples.

The fourth crystal studied was smaller (0·25 × 0·25 × 0·15 mm); we hoped the reduced size might minimize problems connected with contraction of the unit cell. We also decided to collect data sets in order of decreasing, rather than increasing, temperature in the hope that any accumulated strain would be dissipated during the several days required for each data set.

Data sets for the fourth crystal were collected at 295, 259, 220, 181, 140 and 94 K, *i.e.*, at intervals of *ca* 40 K. Temperatures were monitored with a chromel–alumel thermocouple positioned in the nitrogen cold stream ahead of the crystal; stability and reproducibility were estimated to be about 1 K at the lower and about 2 K at the higher temperatures. Previous calibrations with a second thermocouple placed at the crystal site have shown that the temperature difference between the two locations is not more than a degree or two.

Between data sets the temperature was lowered over a period of 1–2 h; the crystal was then allowed to equilibrate and stabilize for about 6 h. Each data set required nearly 4 days, during which the average reflection WIDTH was constant. The average WIDTH did increase in a regular manner as the temperature was lowered, from *ca* 0·20° at 295 K to *ca* 0·36° at 94 K. Some peaks broadened more than others, but the matter was not pursued. At the end of data collection the crystal was examined again under a microscope. Several fault planes were observed, but they were not as conspicuous as in the larger crystal.

Cell constants (see Table 1 and Fig. 1) were determined from the setting angles of 10 sets of Friedel pairs, each pair having $10 < \theta < 19°$ (20 reflections in all). For the sake of consistency the $P2_1/a$ orientation used by most authors was retained. The cell constants were determined both at the beginning and at the end of data collection. The values of the angles α and γ never differed from 90° by more than 0·04°, and in all cases but two the difference was less than 0·02°. The estimated standard deviations (hereafter, e.s.d.'s) for the angles α and γ averaged 0·015°.

Intensities of all reflections having h, $k \geq 0$ were measured with ω scans. The scan width, not including the extensions for the background measurements, was increased from 1·2° at 295 K to 1·4° at 140 K and 1·5° at 94 K (the scan width for the larger crystal was 1·7° at all temperatures). The maximum time spent measuring any reflection was 200 s; for stronger reflections this time was reduced as much as possible consistent with the condition $[\sigma(I)/I] < 0{\cdot}02$. For the two data sets measured at 94 K, $\theta_{max} = 30{\cdot}0°$

Table 1. *Lattice dimensions for anthracene at six temperatures*

T (K)	a (Å)	b (Å)	c (Å)	β (°)	V (Å^3)
Third (larger) crystal					
94	8·4260 (15)	5·9830 (12)	11·0968 (26)	125·328 (19)	456·4 (2)
Fourth (smaller) crystal					
94	8·4144 (20)	5·9903 (14)	11·0953 (17)	125·293 (18)	456·5 (2)
140	8·4414 (15)	5·9958 (15)	11·1123 (13)	125·175 (14)	459·7 (2)
181	8·4673 (18)	5·9994 (17)	11·1244 (17)	125·056 (18)	462·6 (2)
220	8·4959 (17)	6·0033 (13)	11·1407 (12)	124·907 (14)	466·0 (2)
259	8·5254 (14)	6·0088 (14)	11·1548 (11)	124·757 (12)	469·5 (2)
295	8·5526 (12)	6·0158 (11)	11·1720 (16)	124·596 (15)	473·2 (2)

($\sin\theta/\lambda < 0{\cdot}70$ Å^{-1}). At all other temperatures $\theta_{max} = 27{\cdot}5°$ ($\sin\theta/\lambda < 0{\cdot}65$ Å^{-1}).

The agreement between the observed and calculated positions of the stronger reflections was monitored continuously during data collection. Only once did the position of the crystal change appreciably (angular shift of more than 0·15°) during the measurement of a data set. About a quarter of the way through the second (259 K) data set the average angular difference between observed and calculated positions of the 20 reflections used to determine the cell constants suddenly jumped from *ca* 0·02 to *ca* 0·20°. The agreement was much worse in some directions than in others (range 0·02 to 0·54°). Once the orientation matrix was redetermined there were no additional problems.

The space-group 'absences', $h0l$ with h odd, were each scanned for 200 s. The only apparent space-group violation was for the 300 reflection, which was well above background at 94, 140 and 181 K. The intensity of this reflection dropped off rapidly, however, with ψ, so we attribute it to multiple scattering rather than to normal Bragg scattering. Most of the reflections $0k0$ with k odd were measured more rapidly, but in no case was any significant intensity observed.

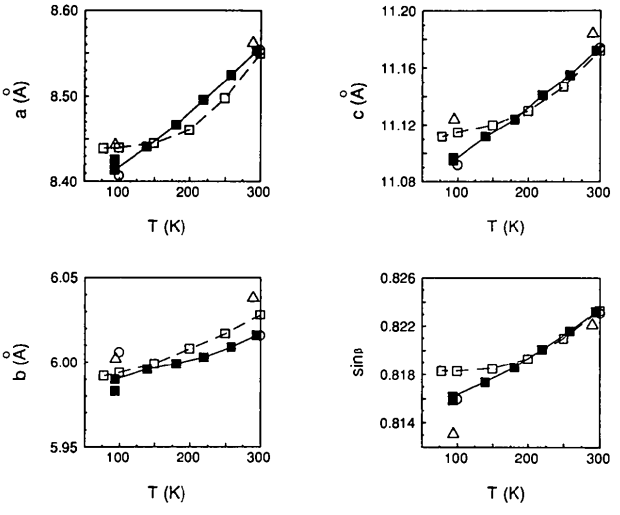

Fig. 1. Temperature dependence of the lattice parameters of anthracene. Values shown include those determined in this study (■; two crystals), as well as those determined by Ryzhenkov, Kozhin & Myasnikova (1969) (□), by Ponomarev & Shilov (1983) (○) and by Mason (1964) (△).

Data were processed using programs of the *XRAY* system (Stewart, Kruger, Ammon, Dickinson & Hall, 1972). There were no measurable changes in the intensities of three control reflections. No correction was made for absorption ($\mu = 0{\cdot}68$ cm^{-1}). Intensities of the approximately 75 pairs of reflections (85 pairs for the two data sets with $\theta_{max} = 30{\cdot}0°$) with indices $0,h,l$ and $0,h,\bar{l}$ were averaged; the R factors (on I) for averaging were all less than 0·02.

The average time required to change the temperature, realign the crystal, and collect data was 3–4 days. The elapsed time required for the seven data sets was 3·7 weeks.

Structure refinement

Full-matrix least-squares refinements based on the reflections having $I > 3\sigma(I)$ started from the coordinates of Mason (1964) and used a locally modified version of the *XRAY* system (Stewart, Kruger, Ammon, Dickinson & Hall, 1972). Since $Z = 2$, each molecule is located on an inversion center. Initially the seven independent C and five independent H atoms were refined isotropically; in later cycles the seven independent C atoms were refined anisotropically. The computer programs used for the final cycles and for the calculation of distances, angles and planes have been described previously (Brock & Webster, 1976); scattering factors were taken from the usual tabulation (Cromer & Waber, 1974). Extinction was judged to be small, so extinction parameters were not included in the final cycles.

Reflection weights used in the initial cycles were derived from counting statistics. After preliminary convergence was obtained, an attempt was made to optimize the weighting scheme using modified weights (Dunitz & Seiler, 1973) following the procedure outlined in the very similar study of naphthalene (Brock & Dunitz, 1982). In that study we could optimize the quality of the refined ADP's (see Fig. 2 in Brock & Dunitz, 1982), as estimated by the rigid-molecule test (Rosenfield, Trueblood & Dunitz, 1978). For anthracene, however, use of modified weights led to no general improvement in the outcome of the test, so a weighting scheme based on counting statistics alone was used. In any event, changing the weighting scheme affects the final values of the components of **L** by less than one e.s.d. The variation in the components of **T** is only a little larger.

There are two noteworthy differences between the results of the naphthalene and anthracene refine-

Table 2. *Some information about the least-squares refinements and* **TL** *fits*

	Data to $\theta = 27{\cdot}5°$							Data to $\theta = 30{\cdot}0°$	
	94 K	140 K	181 K	220 K	259 K	295 K	94 K*	94 K	94 K*
N_{tot}	1045	1057	1063	1069	1075	1085	1054	1325	1329
N_{obs}	690	667	655	610	546	576	846	819	1031
N_v	84	84	84	84	84	84	84	84	84
R	0·040	0·039	0·039	0·037	0·035	0·044	0·048	0·043	0·050
wR	0·041	0·039	0·038	0·034	0·033	0·036	0·056	0·045	0·058
Goodness of fit	2·34	2·31	2·25	2·01	1·94	1·90	3·64	2·42	3·59
$(\Delta/\sigma)_{max}$	0·00	0·00	0·01	0·01	0·01	0·01	0·00	0·00	0·00
Peaks in difference Fourier	+0·33	+0·25	+0·25	+0·16	+0·11	+0·12	+0·56	+0·44	+0·72
(e Å^{-3})	−0·21	−0·24	−0·21	−0·21	−0·19	−0·29	−0·31	−0·90	−0·67
$\langle\Delta^2(A,B)\rangle^{1/2}$ (Å^2)	0·0013	0·0018	0·0022	0·0028	0·0029	0·0035	0·0012	0·0010	0·0009
$\langle\sigma(U^{ij})\rangle$ (Å^2)	0·0008	0·0009	0·0009	0·0009	0·0011	0·0012	0·0007	0·0008	0·0006
R.m.s. $\Delta(U^{ij})$ (Å^2)	0·0007	0·0008	0·0009	0·0011	0·0011	0·0012	0·0006	0·0006	0·0004

* Larger crystal.

ments. First, the e.s.d.'s of the individual U^{ij} values are almost twice as large for anthracene as for naphthalene at comparable reduced temperatures T/T_{mp}. Secondly, an apparently anomalous temperature dependence of the components of the **L** tensor is observed for anthracene (see below). Either of these factors, but especially the second, could account for the different behavior of the two sets of data with respect to weighting scheme.

An attempt was made to refine the structure at 94 K with the high-angle data ($0{\cdot}50 < \sin\theta/\lambda < 0{\cdot}70$ Å^{-1}) from the larger crystal (615 reflections having $I > 0$). The refinement was somewhat unstable and several of the resulting C—H distances were too short [*e.g.*, C(1)—H(1), 0·62 Å]. The 94 K data are evidently not good enough to support a high-angle refinement.

Some information about the final refinements is given in Table 2. The final positional and displacement parameters are listed in Table 3; the atom-numbering scheme is shown in Fig. 2 (note that it does not correspond to the standard chemical numbering).* Bond lengths and angles for the two refinements at 94 K with $\theta_{max} = 30{\cdot}0°$ are listed in an abbreviated version of Table 4; a full version of Table 4 containing distances and angles for all the refinements has been deposited. The e.s.d.'s associated with the C—C bond lengths are 0·002–0·003 Å, indicating that the structures are well determined as judged by normal criteria.

Molecular geometry

The C—C bonds (see Table 4) shorten systematically as the temperature is raised, but this effect nearly disappears when corrections are made for the effects of molecular libration (Dunitz, Schomaker & Trueblood, 1988). The averages over the corrected distances determined for the smaller crystal at six temperatures ($\theta_{max} = 27{\cdot}5°$) are nearly the same as the averages over the two crystals at 94 K ($\theta_{max} = 30{\cdot}0°$).

The C—C bond lengths (corrected for libration) and the bond angles (libration correction negligible) determined at 94 K ($\theta_{max} = 30{\cdot}0°$) have been averaged further under the assumption of molecular $2/m$ symmetry; the results are shown in Fig. 2. The agreement of these C—C distances with those reported previously and with those derived by Pauling (1960, 1980) is remarkable (see Table 5). The root-mean-square (hereafter, r.m.s.) differences between the distances determined in the current study and in the older studies are consistent with the e.s.d.'s. The C—C distances determined in this study, however, cannot be viewed as definitive; no matter how precise bond lengths may appear, they cannot

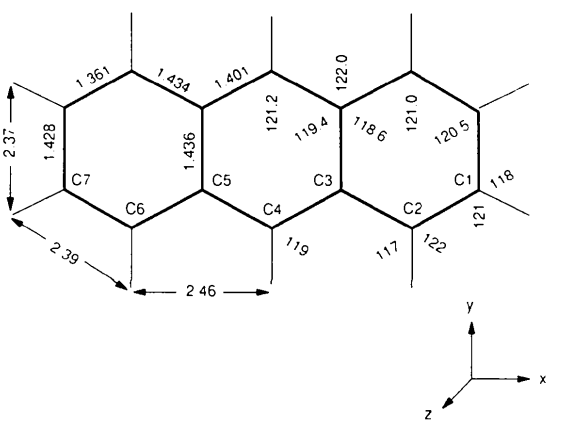

Fig. 2. Diagram of the anthracene molecule showing the atom-numbering scheme and some bond lengths (Å) and angles (°); the axes of the inertial system are also shown. The distances and angles were determined at 94 K with data having $\theta_{max} = 30°$; the distances were corrected for the effects of libration, and the distances and angles were then averaged over the two determinations and over the molecular $2/m$ symmetry.

* Lists of observed and calculated structure-factor amplitudes, bond lengths and angles, and **T** and **L** tensors determined in the Cartesian crystal and inertial coordinate systems have been deposited with the British Library Document Supply Centre as Supplementary Publication No. SUP 53358 (54 pp.). Copies may be obtained through The Technical Editor, International Union of Crystallography, 5 Abbey Square, Chester CH1 2HU, England.

Table 3. *Positional and vibrational parameters* (Å^2) (C *atoms* $\times 10^4$; H *atoms* $\times 10^3$) *for anthracene at six temperatures*

The form of the anisotropic displacement expression is: $\exp[-2\pi^2(U_{11}h^2a^{*2} + U_{22}k^2b^{*2} + U_{33}l^2c^{*2} + 2U_{12}hka^*b^* + 2U_{13}hla^*c^* + 2U_{23}klb^*c^*)]$.

	x	y	z	U^{11}	U^{22}	U^{33}	U^{12}	U^{13}	U^{23}
94 K									
C(1)	861 (3)	266 (3)	3681 (2)	183 (9)	224 (10)	152 (8)	12 (8)	87 (8)	−16 (7)
C(2)	1172 (2)	1555 (3)	2830 (2)	141 (9)	162 (10)	168 (8)	8 (8)	69 (7)	−27 (7)
C(3)	585 (2)	814 (3)	1398 (2)	100 (8)	129 (9)	149 (8)	16 (7)	56 (7)	−2 (7)
C(4)	870 (2)	2111 (3)	491 (2)	114 (8)	108 (9)	174 (8)	5 (7)	66 (7)	−4 (7)
C(5)	307 (2)	1343 (3)	−896 (2)	94 (8)	117 (9)	158 (8)	15 (7)	57 (7)	7 (7)
C(6)	602 (2)	2643 (3)	−1834 (2)	124 (9)	150 (10)	194 (8)	−3 (8)	77 (7)	17 (7)
C(7)	49 (3)	1863 (3)	−3174 (2)	165 (9)	207 (10)	198 (9)	21 (8)	107 (8)	50 (7)
H(1)	123 (3)	76 (3)	466 (2)	25 (5)					
H(2)	184 (2)	302 (3)	319 (2)	17 (5)					
H(4)	151 (3)	354 (3)	85 (2)	16 (5)					
H(6)	124 (2)	410 (3)	−145 (2)	16 (5)					
H(7)	33 (2)	276 (3)	−380 (2)	22 (5)					
140 K									
C(1)	864 (3)	270 (3)	3675 (2)	262 (10)	328 (12)	211 (9)	14 (9)	128 (8)	−21 (8)
C(2)	1172 (2)	1554 (3)	2824 (2)	215 (9)	226 (11)	219 (9)	10 (8)	102 (8)	−32 (8)
C(3)	586 (2)	816 (3)	1394 (2)	145 (8)	186 (10)	205 (9)	18 (7)	85 (7)	−4 (7)
C(4)	871 (2)	2105 (3)	490 (2)	163 (9)	154 (9)	233 (9)	−9 (7)	90 (7)	−12 (7)
C(5)	305 (2)	1338 (3)	−896 (2)	131 (8)	169 (10)	209 (8)	21 (7)	80 (7)	11 (7)
C(6)	601 (2)	2631 (3)	−1831 (2)	179 (9)	227 (11)	274 (9)	1 (8)	118 (8)	33 (8)
C(7)	47 (3)	1851 (4)	−3169 (2)	247 (10)	321 (12)	257 (9)	22 (9)	152 (8)	72 (8)
H(1)	122 (3)	74 (3)	466 (2)	37 (5)					
H(2)	180 (2)	303 (3)	316 (2)	21 (5)					
H(4)	151 (3)	355 (3)	86 (2)	24 (5)					
H(6)	123 (2)	413 (3)	−148 (2)	24 (5)					
H(7)	28 (3)	277 (3)	−380 (2)	36 (5)					
181 K									
C(1)	865 (3)	276 (3)	3667 (2)	342 (10)	439 (13)	264 (9)	24 (10)	166 (9)	−23 (9)
C(2)	1174 (2)	1553 (3)	2819 (2)	271 (10)	306 (11)	274 (9)	8 (8)	127 (8)	−44 (8)
C(3)	586 (2)	815 (3)	1392 (2)	184 (8)	237 (10)	256 (9)	14 (7)	104 (7)	−14 (7)
C(4)	873 (2)	2097 (3)	486 (2)	209 (9)	202 (9)	300 (9)	1 (7)	122 (7)	−11 (7)
C(5)	306 (2)	1332 (3)	−895 (2)	183 (8)	221 (9)	271 (8)	24 (7)	114 (7)	22 (7)
C(6)	600 (2)	2619 (3)	−1832 (2)	245 (9)	273 (11)	346 (9)	−5 (8)	157 (8)	35 (8)
C(7)	46 (3)	1845 (3)	−3166 (2)	319 (10)	408 (12)	321 (9)	25 (9)	192 (9)	83 (9)
H(1)	123 (2)	78 (3)	463 (2)	39 (5)					
H(2)	181 (2)	301 (3)	316 (2)	34 (5)					
H(4)	152 (2)	353 (3)	84 (2)	31 (5)					
H(6)	123 (2)	409 (3)	−146 (2)	25 (4)					
H(7)	30 (2)	275 (3)	−380 (2)	43 (5)					
220 K									
C(1)	866 (3)	282 (3)	3661 (2)	430 (11)	543 (14)	331 (10)	26 (10)	215 (10)	−27 (9)
C(2)	1175 (2)	1552 (3)	2811 (2)	346 (10)	376 (11)	344 (10)	9 (9)	175 (9)	−46 (9)
C(3)	588 (2)	818 (3)	1390 (2)	236 (9)	272 (10)	321 (9)	15 (7)	139 (8)	−16 (7)
C(4)	874 (2)	2092 (3)	484 (2)	254 (9)	242 (10)	374 (9)	−4 (7)	150 (8)	−18 (7)
C(5)	306 (2)	1327 (3)	−896 (2)	226 (8)	269 (9)	335 (9)	12 (8)	152 (8)	14 (7)
C(6)	600 (2)	2610 (3)	−1832 (2)	294 (10)	357 (11)	430 (10)	−3 (9)	198 (9)	46 (9)
C(7)	43 (3)	1829 (4)	−3163 (2)	407 (11)	510 (13)	389 (10)	27 (10)	244 (9)	93 (9)
H(1)	130 (2)	79 (3)	466 (2)	50 (5)					
H(2)	183 (2)	302 (3)	315 (2)	46 (5)					
H(4)	149 (2)	353 (3)	82 (2)	40 (5)					
H(6)	124 (2)	408 (3)	−147 (2)	39 (5)					
H(7)	25 (2)	275 (3)	−384 (2)	58 (6)					
259 K									
C(1)	866 (3)	290 (4)	3652 (2)	518 (13)	627 (16)	395 (11)	3 (12)	245 (11)	−35 (11)
C(2)	1175 (3)	1555 (4)	2805 (2)	419 (11)	447 (13)	425 (11)	10 (10)	211 (9)	−51 (10)
C(3)	590 (2)	816 (3)	1388 (2)	288 (9)	327 (11)	381 (10)	20 (8)	173 (8)	−14 (9)
C(4)	875 (2)	2084 (3)	482 (2)	312 (10)	287 (11)	440 (10)	−10 (9)	178 (8)	−24 (9)
C(5)	304 (2)	1319 (3)	−896 (2)	271 (9)	318 (11)	406 (10)	25 (8)	184 (8)	25 (8)
C(6)	600 (3)	2593 (4)	−1832 (2)	356 (11)	442 (14)	506 (11)	−8 (11)	233 (9)	57 (11)
C(7)	38 (3)	1817 (4)	−3161 (2)	491 (12)	622 (16)	473 (11)	26 (12)	295 (10)	108 (11)
H(1)	132 (2)	79 (3)	465 (2)	59 (6)					
H(2)	182 (3)	300 (3)	312 (2)	57 (6)					
H(4)	150 (3)	355 (3)	81 (2)	48 (5)					
H(6)	123 (2)	406 (3)	−146 (2)	47 (5)					
H(7)	25 (3)	272 (4)	−383 (2)	73 (6)					
295 K									
C(1)	867 (3)	288 (4)	3644 (3)	620 (15)	748 (19)	466 (14)	32 (14)	302 (13)	−45 (13)
C(2)	1178 (3)	1555 (4)	2798 (2)	508 (14)	529 (15)	499 (13)	−4 (12)	257 (11)	−74 (12)
C(3)	589 (2)	817 (3)	1384 (2)	338 (11)	370 (13)	460 (12)	22 (9)	209 (10)	−16 (10)
C(4)	875 (2)	2074 (4)	477 (2)	355 (11)	339 (13)	518 (12)	−17 (10)	209 (10)	−32 (10)
C(5)	303 (2)	1314 (3)	−896 (2)	329 (10)	356 (12)	470 (11)	19 (9)	214 (9)	33 (9)
C(6)	601 (3)	2577 (4)	−1830 (2)	425 (12)	510 (15)	570 (13)	10 (12)	260 (11)	61 (12)
C(7)	35 (3)	1806 (4)	−3156 (2)	563 (14)	712 (18)	563 (14)	31 (14)	339 (12)	137 (13)
H(1)	127 (3)	82 (3)	459 (2)	64 (6)					
H(2)	182 (3)	297 (4)	313 (2)	64 (7)					
H(4)	151 (3)	350 (3)	82 (2)	50 (5)					

Table 3 (*cont.*)

	x	y	z	U^{11}	U^{22}	U^{33}	U^{12}	U^{13}	U^{23}
H(6)	123 (2)	405 (3)	−147 (2)	54 (6)					
H(7)	27 (3)	271 (4)	−380 (2)	84 (7)					
94 K (larger crystal)									
C(1)	866 (2)	267 (3)	3686 (2)	185 (8)	193 (9)	190 (8)	18 (7)	109 (7)	−11 (6)
C(2)	1171 (2)	1554 (3)	2828 (2)	148 (8)	137 (8)	195 (8)	2 (6)	95 (7)	−31 (6)
C(3)	588 (2)	817 (3)	1400 (2)	106 (7)	98 (8)	181 (8)	16 (6)	80 (6)	−2 (6)
C(4)	869 (2)	2112 (2)	489 (2)	117 (8)	83 (8)	196 (8)	−2 (6)	83 (6)	−7 (6)
C(5)	308 (2)	1342 (2)	−894 (2)	100 (8)	91 (8)	182 (8)	16 (6)	79 (7)	14 (6)
C(6)	602 (2)	2644 (3)	−1833 (2)	133 (8)	121 (8)	223 (8)	3 (6)	102 (7)	20 (6)
C(7)	53 (2)	1863 (3)	−3172 (2)	172 (8)	180 (8)	222 (8)	6 (7)	129 (7)	41 (6)
H(1)	129 (2)	75 (3)	470 (2)	21 (5)					
H(2)	187 (3)	300 (4)	320 (2)	23 (5)					
H(4)	154 (3)	354 (3)	87 (2)	18 (4)					
H(6)	125 (3)	405 (3)	−145 (2)	22 (5)					
H(7)	30 (3)	277 (4)	−381 (2)	27 (5)					
94 K (smaller crystal; data to $\theta = 30{\cdot}0°$)									
C(1)	860 (3)	267 (3)	3682 (2)	183 (8)	208 (10)	151 (8)	9 (8)	92 (7)	−14 (7)
C(2)	1173 (2)	1556 (3)	2830 (2)	142 (8)	159 (9)	157 (8)	6 (7)	69 (7)	−27 (7)
C(3)	585 (2)	814 (3)	1398 (2)	105 (8)	116 (9)	143 (8)	7 (6)	59 (7)	−1 (6)
C(4)	871 (2)	2114 (3)	492 (2)	120 (8)	105 (9)	159 (8)	3 (7)	69 (7)	−5 (6)
C(5)	306 (2)	1342 (3)	−896 (2)	99 (8)	110 (9)	143 (7)	9 (7)	61 (7)	5 (6)
C(6)	604 (2)	2646 (3)	−1833 (2)	125 (8)	146 (9)	184 (8)	−6 (7)	80 (7)	21 (7)
C(7)	49 (3)	1864 (3)	−3175 (2)	173 (9)	201 (10)	184 (8)	14 (8)	108 (7)	42 (7)
H(1)	122 (3)	75 (3)	466 (2)	25 (5)					
H(2)	184 (3)	302 (3)	319 (2)	16 (5)					
H(4)	152 (3)	353 (3)	86 (2)	16 (5)					
H(6)	124 (2)	409 (3)	−146 (2)	16 (5)					
H(7)	33 (3)	275 (3)	−380 (2)	22 (5)					
94 K (larger crystal; data to $\theta = 30{\cdot}0°$)									
C(1)	866 (2)	266 (3)	3687 (2)	181 (7)	184 (8)	178 (7)	15 (6)	107 (6)	−8 (6)
C(2)	1172 (2)	1556 (3)	2828 (2)	148 (7)	134 (7)	178 (7)	−1 (6)	91 (6)	−29 (5)
C(3)	587 (2)	816 (2)	1400 (2)	109 (6)	91 (6)	164 (7)	9 (5)	78 (5)	−2 (5)
C(4)	870 (2)	2115 (2)	490 (2)	119 (7)	80 (7)	178 (7)	−4 (5)	82 (6)	−6 (5)
C(5)	307 (2)	1342 (2)	−895 (2)	102 (7)	85 (7)	164 (6)	8 (5)	77 (6)	12 (5)
C(6)	603 (2)	2646 (3)	−1833 (2)	131 (7)	118 (7)	207 (7)	−3 (5)	100 (6)	19 (6)
C(7)	52 (2)	1864 (3)	−3174 (2)	171 (7)	176 (7)	202 (7)	5 (6)	122 (6)	36 (6)
H(1)	129 (2)	75 (3)	470 (2)	23 (4)					
H(2)	188 (2)	301 (3)	321 (2)	22 (5)					
H(4)	154 (3)	354 (3)	87 (2)	19 (4)					
H(6)	125 (2)	405 (3)	−145 (2)	21 (5)					
H(7)	29 (3)	277 (3)	−382 (2)	27 (5)					

be determined to better than 0·01 Å by low-order ($\sin\theta/\lambda < 0{\cdot}65$ Å^{-1}) diffraction data using spherical free-atom-scattering factors (Seiler, Schweizer & Dunitz, 1984). An attempt to rectify this deficiency has been made (Brock, Dunitz & Hirshfeld, 1991). This attempt involves new refinements in which the free-atom-scattering factors are augmented by multipole expansion terms transferred from an electron-density study of perylene (Hirshfeld, Hope & Rabinovich, 1990). The C—C distances so obtained (see Table 5) are probably the best currently available and suggest that the C(1)—C(2) and C(6)—C(7) bond lengths derived from the present study are about 0·01 Å too short.

The H—C—C bond angles in Table 4 and in Fig. 2 show that the H(2) and H(6) atoms tilt slightly towards the center of the molecule so that the H···H distances around the periphery of the molecule are more nearly balanced.

The deviations of the C atoms from the mean molecular plane have e.s.d.'s of 0·002 Å and do not exceed 0·010 Å at any temperature (r.m.s. value 0·006 Å); the corresponding deviations of the H atoms are as large as 0·07 Å.

Analysis of anisotropic displacement parameters

The crystallographically determined U^{ij} values were analyzed using Trueblood's program *THMA*11 (Trueblood, 1978; Dunitz, Schomaker & Trueblood, 1988). The 12 components of the molecular translational (**T**) and librational (**L**) tensors were determined in a linear least-squares procedure from the 42 U^{ij} values determined for the seven independent C atoms. (The correlation tensor **S** vanishes as a result of the crystallographic site symmetry *i*.) Three different fits were made. The first fit was of the experimental U^{ij}'s in the Cartesian crystal system ($\mathbf{x}_1||\mathbf{a}$, $\mathbf{x}_2||\mathbf{b}$, $\mathbf{x}_3||\mathbf{c}^*$) with weights proportional to $[\sigma(U^{ij})]^{-2}$ (the tensors have been deposited†). The second was an unweighted fit of the transformed U^{ij}'s in the inertial coordinate system (the axial system is shown in Fig. 2‡). This fit has the advan-

† See deposition footnote.

‡ The axial system shown in Fig. 2 is the same as the system chosen by Cruickshank (1956*a*). The directions of the **x** and **z** axes in the system used by *THMA*11 happen to be reversed relative to Cruickshank's system. Values of T^{12}_{int}, T^{23}_{int}, L^{12}_{int}, and L^{23}_{int} calculated by *THMA*11 are therefore here reversed in sign to make them consistent with the coordinate system shown.

Table 4. *Bond lengths* (Å) *and angles* (°) *refined for anthracene at* 94 K *with data to* $\theta = 30{\cdot}0°$

	Smaller crystal	Larger crystal
C(1)—C(2)	1·358 (2)	1·362 (2)
C(2)—C(3)	1·435 (2)	1·431 (2)
C(3)—C(4)	1·399 (2)	1·400 (2)
C(3)—C(5)′	1·434 (2)	1·436 (2)
C(4)—C(5)	1·402 (2)	1·399 (2)
C(5)—C(6)	1·433 (2)	1·433 (2)
C(6)—C(7)	1·361 (2)	1·360 (2)
C(7)—C(1)′	1·426 (3)	1·427 (2)
C(1)—H(1)	0·99 (2)	1·01 (2)
C(2)—H(2)	0·99 (2)	1·00 (2)
C(4)—H(4)	0·96 (2)	0·98 (2)
C(6)—H(6)	0·98 (2)	0·95 (2)
C(7)—H(7)	1·00 (2)	1·01 (2)
C(7)′—C(1)—C(2)	120·7 (2)	120·3 (1)
C(1)—C(2)—C(3)	120·9 (2)	121·1 (1)
C(2)—C(3)—C(4)	122·1 (2)	122·3 (1)
C(2)—C(3)—C(5)′	118·5 (1)	118·5 (1)
C(4)—C(3)—C(5)′	119·4 (1)	119·2 (1)
C(3)—C(4)—C(5)	121·1 (2)	121·2 (1)
C(4)—C(5)—C(6)	121·7 (2)	121·8 (1)
C(4)—C(5)—C(3)′	119·5 (1)	119·6 (1)
C(6)—C(5)—C(3)′	118·7 (1)	118·6 (1)
C(5)—C(6)—C(7)	120·8 (2)	121·0 (1)
C(6)—C(7)—C(1)′	120·4 (2)	120·5 (1)
H(1)—C(1)—C(7)′	116·6 (11)	117·5 (10)
H(1)—C(1)—C(2)	122·7 (12)	122·2 (10)
H(2)—C(2)—C(1)	120·8 (10)	120·5 (9)
H(2)—C(2)—C(3)	118·3 (10)	118·4 (9)
H(4)—C(4)—C(3)	118·7 (10)	118·1 (10)
H(4)—C(4)—C(5)	120·2 (10)	120·6 (10)
H(6)—C(6)—C(5)	117·2 (10)	116·5 (10)
H(6)—C(6)—C(7)	122·0 (10)	122·4 (10)
H(7)—C(7)—C(6)	120·2 (11)	120·6 (11)
H(7)—C(7)—C(1)′	119·3 (11)	118·9 (11)
H(1)···H(2)	2·40 (3)	2·40 (3)
H(2)···H(4)	2·46 (2)	2·46 (2)
H(4)···H(6)	2·46 (2)	2·46 (2)
H(6)···H(7)	2·38 (2)	2·38 (2)
H(7)···H(1)′	2·36 (3)	2·38 (3)

tage of providing e.s.d.'s of T^{ij} and L^{ij} components along inertial axes. (These e.s.d's are not provided by *THMA*11 when the input is in the crystal system.) The $\sigma(U^{ij})$ values vary little across the 42 observations, so the results of the weighted and unweighted fits are similar.

The third fit (unweighted, inertial system) was performed after correction of the U^{ij} values for the effects of internal motion. The general procedure was similar to that described previously for naphthalene (Brock & Dunitz, 1982). The contributions to U^{ij} from the $3(14 + 10) - 6 = 66$ intramolecular modes were calculated by Cyvin (1981) for an isolated anthracene molecule at six temperatures. The normal-coordinate calculation (Cyvin, Cyvin, Hagen, Cruickshank & Pawley, 1972) was based on a general force field for in the in-plane (Bakke, Cyvin, Whitmer, Cyvin, Gustavsen & Klaeboe, 1979) and out-of-plane (Neerland, Cyvin, Brunvoll, Cyvin & Klaeboe, 1980) vibrations of aromatic molecules. The values of the correction terms U^{ij}_{intra} for the temperatures corresponding to the crystal structure determinations were obtained by linear interpolation of Cyvin's (1981) values (see Table 6). The results after this

Table 5. *Comparison of average* C—C *bond lengths* (Å) *determined in several studies*

	P[c]	B&D[d]	C&S[e]	CSD[f]	BD&H[g]
C(1)—C(7)′	1·439	1·428	1·419	1·415 (12)	1·431
C(1)—C(2)	1·361	1·361	1·368	1·366 (7)	1·369
C(2)—C(3)	1·439	1·434	1·436	1·432 (8)	1·434
C(3)—C(5)′	1·439	1·436	1·428	1·433 (6)	1·441
C(3)—C(4)	1·394	1·401	1·399	1·399 (6)	1·403
E.s.d.[a]		0·001	0·004		<0·001
R.m.s. (Δ)[b]	0·007	0·005	0·008	0·008	

Notes: (*a*) Average estimated standard deviation for bond lengths as provided by authors. (*b*) Root-mean-square difference relative to values determined by BD&H. (*c*) Pauling (1960), predicted bond lengths. (*d*) This study, values corrected for libration. (*e*) Cruickshank & Sparks (1960), values corrected for libration and averaged over several studies. (*f*) Averages obtained by routine search of the July 1988 version of the Cambridge Structural Database (Allen *et al.*, 1979) and analysis of the seven hits; estimated standard deviations in parentheses measure the widths of the distributions. Studies included were those by Lehmann & Pawley (1972) ($C_{14}H_{10}$), Mason (1964) (295 and 90 K), Mathieson, Robertson & Sinclair (1950), Cruickshank (1956*a*) and Ponomarev & Shilov (1983) (300 and 100 K). (*g*) Brock, Dunitz & Hirshfeld (1991), values derived from refinements in which the spherical scattering factors for the C and H atoms were augmented by multiple expansions to account for bonding effects. The refinements included libration corrections and the values given have been averaged over the six temperatures.

Table 6. *Mean-square amplitudes* U^{ij} (Å^2) *of internal vibration calculated for the chemically independent* C *atoms of anthracene along the inertial axes* (*see Fig.* 2)

Linear interpolations from values calculated at 100, 150, 200, 250 and 300 K by Cyvin (1981). For C(5), C(6) and C(7) the quantity given is $-U^{12}$ rather than U^{12}.

T	U^{11}	U^{22}	U^{33}	U^{12}	U^{13}	U^{23}
C(1); C(7)						
94 K	0·00162	0·00139	0·00458	0·00004	0	0
140 K	0·00165	0·00145	0·00554	0·00006	0	0
181 K	0·00170	0·00153	0·00654	0·00009	0	0
220 K	0·00175	0·00162	0·00755	0·00013	0	0
259 K	0·00182	0·00171	0·00859	0·00016	0	0
295 K	0·00190	0·00181	0·00957	0·00019	0	0
C(2); C(6)						
94 K	0·00169	0·00136	0·00358	−0·00013	0	0
140 K	0·00176	0·00136	0·00411	−0·00013	0	0
181 K	0·00183	0·00137	0·00470	−0·00013	0	0
220 K	0·00191	0·00140	0·00530	−0·00013	0	0
259 K	0·00202	0·00143	0·00594	−0·00014	0	0
295 K	0·00213	0·00146	0·00656	−0·00015	0	0
C(3); C(5)						
94 K	0·00127	0·00153	0·00378	−0·00008	0	0
140 K	0·00128	0·00158	0·00432	−0·00009	0	0
181 K	0·00129	0·00164	0·00492	−0·00010	0	0
220 K	0·00132	0·00171	0·00552	−0·00011	0	0
259 K	0·00135	0·00179	0·00616	−0·00013	0	0
295 K	0·00138	0·00188	0·00678	−0·00015	0	0
C(4)						
94 K	0·00142	0·00178	0·00433	0·00000	0	0
140 K	0·00143	0·00183	0·00508	0·00000	0	0
181 K	0·00144	0·00190	0·00589	0·00000	0	0
220 K	0·00147	0·00199	0·00671	0·00000	0	0
259 K	0·00150	0·00209	0·00757	0·00000	0	0
295 K	0·00153	0·00220	0·00839	0·00000	0	0

correction are shown in Tables 7 and 8. The eigenvalues and eigenvectors for the **L** tensors (hereafter designated $\mathbf{L}_{\text{int}}$) are given in Table 9; the eigenvectors for the **T** tensors are essentially coincident with the internal axes.

Table 7. *Components of* **T** ($Å^2 \times 10^4$) *and* **L** (deg^2) *determined for the smaller crystal in the inertial coordinate system defined in Fig. 2 after correction for internal motion*

	T			L		
94 K						
167 (4)	2 (4)	−7 (5)	4·6 (20)	0·4 (3)	0·6 (6)	
	92 (6)	−1 (6)		2·0 (3)	−0·3 (2)	
		37 (11)			2·9 (2)	
140 K						
220 (6)	0 (6)	6 (6)	7·2 (26)	0·6 (4)	1·2 (7)	
	134 (8)	1 (8)		3·0 (4)	−0·4 (3)	
		64 (14)			4·5 (3)	
181 K						
279 (6)	3 (6)	−8 (7)	8·0 (31)	0·5 (4)	0·9 (8)	
	178 (9)	0 (9)		3·9 (4)	−0·6 (4)	
		98 (16)			5·8 (4)	
220 K						
337 (7)	0 (7)	1 (8)	8·0 (33)	0·8 (5)	1·5 (9)	
	216 (10)	2 (10)		4·9 (5)	−0·7 (4)	
		136 (18)			7·4 (4)	
259 K						
409 (8)	−4 (8)	−3 (9)	11·1 (39)	1·0 (6)	−2·0 (11)	
	267 (12)	1 (12)		6·3 (6)	−1·0 (5)	
		162 (21)			8·3 (5)	
295 K						
477 (9)	−4 (9)	0 (10)	15·3 (43)	1·4 (6)	2·5 (12)	
	302 (13)	−2 (13)		7·2 (6)	−1·1 (5)	
		194 (23)			10·3 (5)	

Table 8. *Components of* **T** ($Å^2 \times 10^4$) *and* **L** (deg^2) *determined at* 94 K *for two different crystals and two different values of* θ_{max} *in the inertial coordinate system defined in Fig. 2 after correction for internal motion*

	$\theta_{max} = 27·5°$			$\theta_{max} = 30·0°$		
Smaller crystal						
T 167 (4)	2 (4)	−7 (5)	149 (4)	0 (3)	−4 (4)	
	92 (6)	−1 (6)		85 (5)	−2 (5)	
		37 (11)			47 (9)	
L 4·6 (20)	0·4 (3)	0·6 (6)	3·6 (16)	0·2 (2)	0·7 (5)	
	2·0 (3)	−0·3 (2)		1·9 (2)	−0·2 (2)	
		2·9 (2)			2·8 (2)	
Larger crystal						
T 176 (4)	−13 (4)	12 (4)	156 (3)	−13 (3)	11 (3)	
	73 (6)	−13 (6)		66 (4)	−12 (4)	
		32 (10)			40 (7)	
L 4·9 (18)	0·2 (3)	0·6 (5)	4·5 (14)	0·2 (2)	0·6 (4)	
	2·0 (3)	−0·3 (2)		1·8 (2)	−0·2 (2)	
		2·8 (2)			2·8 (2)	

Table 9. *Eigenvalues of* **L** (deg^2) *and associated eigenvectors in the inertial coordinate system after correction for internal motion*

	$\theta_{max} = 27·5°$			$\theta_{max} = 30·0°$		
94 K (smaller crystal)						
4·8	0·95	0·10	0·30	4·0	0·88	0·05	0·48
2·9	0·25	0·36	−0·90	2·6	0·42	0·40	−0·81
1·8	0·20	−0·93	−0·32	1·7	0·23	−0·92	−0·33
140 K							
7·7	0·93	0·08	0·35				
4·3	0·29	0·41	−0·87				
2·8	0·21	−0·91	−0·36				
181 K							
8·3	0·95	0·07	0·31				
5·8	0·26	0·35	−0·90				
3·6	0·17	−0·94	−0·31				
220 K							
9·2	0·78	0·04	0·62				
6·7	0·53	0·48	−0·70				
4·3	0·33	−0·88	−0·35				
259 K							
12·1	0·89	0·09	0·44				
8·2	0·32	0·56	−0·76				
5·4	0·31	−0·82	−0·47				
295 K							
16·4	0·93	0·09	0·36				
10·1	0·28	0·46	−0·84				
6·3	0·24	−0·88	−0·40				
94 K (larger crystal)							
5·1	0·97	0·05	0·24	4·7	0·95	0·05	0·29
2·8	0·21	0·37	−0·91	2·7	0·26	0·33	−0·91
1·9	0·14	−0·93	−0·35	1·7	0·14	−0·94	−0·30

The results of the various analyses are displayed in Figs. 3 and 4. Fig. 3 shows the temperature dependence of the diagonal components of **T** and **L** in the Cartesian crystal system. Diagonal components, rather than eigenvalues, are displayed because e.s.d.'s are available for the former, but not for the latter. Fig. 4 shows the temperature dependence of the diagonal components in the inertial system, both with and without correction for the contributions of the internal modes. For a harmonic mean-field potential the T^{ii} and L^{ii} values should increase approximately linearly with temperature (see *e.g.* Dunitz, Schomaker & Trueblood, 1988). For a crystal like anthracene that expands with temperature, the plots of the diagonal components *versus* T should have a positive second derivative. These expectations are fulfilled for **T** but not for **L**. A comparison of Figs. 3 and 4 reveals that the anomalous contraction of the **L** tensor as the temperature is lowered is concentrated in L^{11}_{int}, the component associated with libration about the long molecular axis. A plot of the eigenvalues shows the same anomaly, although it is not quite as pronounced.

Fig. 4 shows that corrections for internal motion have little effect on the temperature dependencies of the T^{ii} and L^{ii} values. The corrections lower all the T^{ii} values; since the out-of-plane modes are the softest, the decrease is largest in the direction perpendicular to the molecular plane. The effect on the L^{ii} values is smaller. In naphthalene (Brock & Dunitz, 1982) the correction for internal motion reversed the order of the L^{11}_{int} and L^{33}_{int} values, but for anthracene $L^{33}_{int} < L^{11}_{int}$ even before correction.

While the **TL** fits are good by all but the highest standards [r.m.s. (ΔU^{ij}) is 0·0006–0·0012 $Å^2$], the discrepancies are about twice as large as in naphthalene. The atomic **U** tensors themselves are not as well determined for anthracene as for naphthalene, the $\sigma(U^{ij})$ being 1·5–2·0 times larger for comparable

values of U^{ii}. For rigid molecules the r.m.s. $\Delta(A,B)^2$ is a good measure of the quality of the **U** tensors (Rosenfield, Trueblood & Dunitz, 1978); it is also about twice as large for anthracene as for naphthalene after refinement with statistical weights (see Table 2).

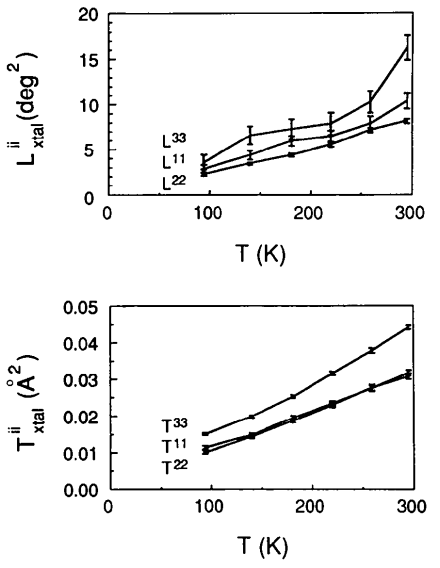

Fig. 3. Diagonal components of **L** and **T** determined for anthracene at six temperatures in the Cartesian crystal coordinate system ($\mathbf{x}_1\|\mathbf{a}$, $\mathbf{x}_2\|\mathbf{b}$, $\mathbf{x}_3\|\mathbf{c}^*$). The lengths of the error bars correspond to one estimated standard deviation.

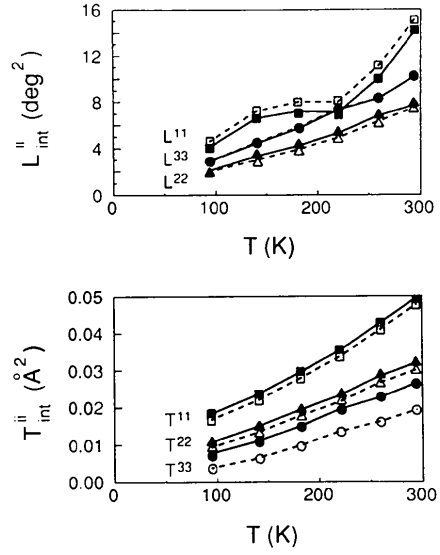

Fig. 4. Diagonal components of **L** and **T** in the inertial coordinate system determined before (solid lines) and after (dashed lines) correction of the U^{ij} values for the effects of the intramolecular modes. The $\mathbf{x}_1$ axis is parallel to the long molecular axis (which has the smallest moment of inertia) and the $\mathbf{x}_3$ axis is perpendicular to the molecular plane.

Fig. 5 displays the 'thermal' ellipsoids for anthracene as determined for the smaller crystal at 92 and 295 K. The general shrinkage with temperature is clear. We might have expected that two of the three principal axes would lie in the molecular plane. This is indeed so, except for C(6), where two axes are inclined to the molecular plane. However, the eigenvalues for **U** tensor of C(6) differ by only 13%, so the directions of the associated eigenvectors are ill-defined.

Discussion

We are left with two questions. (1) Why are the anthracene U^{ij}'s associated with large e.s.d.'s and larger $\Delta(A,B)^2$'s as compared with naphthalene? (2) Is the apparent anomaly in L^{11}_{int} real, and, if so, to what is it to be ascribed?

The reason for the larger $\sigma(U^{ij})$'s in anthracene as compared with naphthalene is not immediately obvious. The intensity data for the two studies were measured in the same way on the same diffractometer at about the same time. If anything, even more care was taken with the anthracene measurements. The widths of the diffraction peaks for the two series of measurements were comparable and changed with temperature in about the same way. The orientation matrices for the two studies were of similar quality. Any errors arising from thermal diffuse scattering should have been about the same for the two substances. The main factor responsible for the lower e.s.d.'s in the naphthalene study is probably the larger crystal size and greater diffracted intensity. The scale factor multiplying F_c was about twice as large for naphthalene as for anthracene. A comparison of the results for the two anthracene crystals studied at 94 K also shows that the larger crystal is associated with slightly smaller e.s.d.'s.

Just as the atomic **U** tensors are less well determined for anthracene than naphthalene, so is

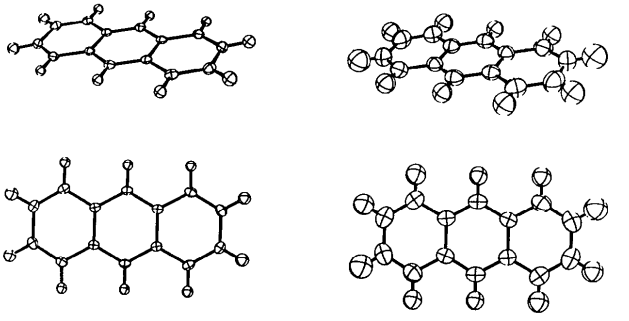

Fig. 5. Perspective views of the anthracene molecule showing the atomic **U** tensors determined at 94 and 295 K (smaller crystal; θ_{max} = 27·5°). The ellipsoids drawn correspond to 50% contours of atomic displacement.

Table 10. *Components of* **T** (Å^2 × 10^4) and **L** (deg^2) *determined in the inertial coordinate system near* 295 K *in various studies*

	Experimental determinations			Lattice-dynamical calculations			
	B&D[a]	C[b]	M[c]	P[d]	VC&D[e]	FGS&S[f]	Cr[g]
T^{11}	477 (9)	380 (16)	480	419	531		667
T^{22}	302 (13)	285 (24)	290	325	316		472
T^{33}	194 (23)	270 (42)	260	272	339		287
T^{12}	−4 (9)	−9 (16)		10	−1		
T^{13}	0 (10)	−9 (18)		−16	4		
T^{23}	−2 (13)	−9 (24)		3	82		
L^{11}	15·3 (43)	15·2 (78)	13·0	15·1	18·8	19·2	16·
L^{22}	7·2 (6)	4·8 (11)	7·3	6·0	6·8	6·9	6·5
L^{33}	10·3 (5)	9·1 (10)	9·6	9·0	11·2	10·6	14·
L^{12}	1·4 (6)	0·8 (11)		1·1	0·7		
L^{13}	2·5 (12)	−4·5 (22)		2·8	2·7		
L^{23}	−1·1 (5)	−0·8 (10)		0·5	0·2		

Notes: (*a*) this study; (*b*) Cruickshank (1956*a*); (*c*) Mason (1964), eigenvalues only; (*d*) Pawley (1967); (*e*) Vovelle, Chedin & Dumas (1978); (*f*) Filippini, Gramaccioli, Simonetta & Suffritti (1973), eigenvalues only; (*g*) Criado (1989), model including charges, eigenvalues only.

the **TL** fit less satisfactory. Because there are more observations for anthracene than napthalene (42 U^{ij} values instead of 30), the values of $\sigma(T^{ii})$ should be about 15% smaller in anthracene, but in fact they are about 2–3 times larger.

The relatively large values of $\sigma(L^{11}_{\rm int})$ for anthracene result from the molecular geometry; the e.s.d.'s are 6–7 times larger than those associated with the other two diagonal components. The corresponding ratio for the naphthalene molecule is 3–4. As discussed by Filippini, Gramaccioli, Simonetta & Suffritti (1974), the apportioning of the error in the **TL** fit among the T^{ij} and L^{ij} components is determined by the structure of the matrix of the normal equations, which in turn depends on the positions of the atoms relative to the inertial axes. The larger the distance of an atom from an inertial axis, the greater its contribution to the corresponding term in the matrix of the normal equations. The larger a diagonal term in this matrix, the smaller the corresponding term in the inverse matrix and the smaller the variance. Thus, while the absolute distances of the atoms from the three axes determine the e.s.d.'s, it is the relative distances that determine their ratio. The value of $L^{11}_{\rm int}$ is more poorly determined in anthracene than naphthalene because the average distances of the atoms from the inertial axis **x** are about the same for the two molecules while the average distances from **y** and **z** (see Fig. 2) are greater for anthracene than naphthalene. In other words, the ratios I^{11}/I^{22} and I^{11}/I^{33} of the principal components of the molecular inertia tensor are substantially smaller for anthracene than for naphthalene.

The effect of the molecular geometry on the quality of the thermal-motion description is striking. Even though the expansion of the **L** tensor is greatest in the direction of the long molecular axis (see Table 7), the ratio of the change in $L^{11}_{\rm int}$ between 94 and 295 K to the average e.s.d. of $L^{11}_{\rm int}$ is only 3. Corresponding ratios for the other five diagonal components are much larger; the ratios are about 12 and 21 for $L^{22}_{\rm int}$ and $L^{33}_{\rm int}$, and are 48, 22 and 9 for $T^{ii}_{\rm int}$, i = 1, 3.

The **TL** fit is at least as good as can be expected given the $\sigma(U^{ij})$'s. The **L** tensors determined at 295 K agree well with those calculated by semi-empirical, lattice-dynamical techniques by Pawley (1967), Filippini, Gramaccioli, Simonetta & Suffritti (1973), Vovelle, Chedin & Dumas (1978) and Criado (1989) (see Table 10). The **T** tensors, which are more likely to be affected by systematic errors, are in qualitative agreement with the calculations. The agreement with thermal-motion descriptions derived from film data (Cruickshank, 1956*a*; Mason, 1964) is also remarkably good (see Table 10).

If the anomalous temperature dependence of $L^{11}_{\rm int}$ were genuine, with what physical process might it be connected? With a molecular reorientation process? Could it arise from incomplete nucleation of a second phase? Although the heat capacity data for anthracene give no indication of a phase transition (Goursot, Girdhar & Westrum, 1968; Ross, Andersson & Bäckström, 1979), much has been written about the possible existence of a second phase (see, *e.g.* Craig, Ogilvie & Reynolds, 1976). Indeed, lattice-energy calculations (Gramaccioli, Filippini, Simonetta, Ramdas, Parkinson & Thomas, 1980; Craig, Ogilvie & Reynolds, 1976; Mirsky & Cohen, 1978) suggest that other anthracene structures are comparable in energy with the known structure, and that some of these alternative structures can be generated from the known structure by motion along slip planes. There are some indications for pressure- and/or stress-driven phase transitions. Parkinson, Goringe, Ramdas, Williams & Thomas (1978) have claimed evidence from transmission electron microscopy for the presence of a stress-induced, triclinic, 'coexistent metastable' phase of anthracene. Adams & Tan (1981) studied the pressure dependence of the mid-range infrared spectrum of anthracene and found discontinuities in the frequency *versus* pressure curves at 24 kbar, which they interpret in terms of a second-order phase transition. Jankowiak, Bässler & Kutoglu (1985) cite unpublished evidence for a molecular reorientation in anthracene at high pressures.

On the other hand, a number of studies have found anthracene to respond normally to variation of temperature and pressure. Nicol, Vernon & Woo (1975) found no evidence of a phase transition in their variable-pressure, variable-temperature Raman study. Nor were any anomalies reported in the Raman spectra of anthracene crystals studied at atmospheric pressure and temperatures of 293, 195,

77 and 4 K (Suzuki, Yokoyama & Ito, 1968). No evidence of a phase change was found in a room-temperature powder diffraction study at hydrostatic pressures up to 0·9 GPa (Pufall & Kalus, 1988), nor in studies by neutron inelastic scattering performed at 14, 100, 200 and 250 K (Dorner *et al.*, 1982; Jindal *et al.*, 1982). While evidence for a phase change can appear in one physical property but not in another, clearly we need to reserve judgement about any connection between the anomalous temperature dependence of $L^{11}_{\rm int}$ and a possible phase transition. In any event, the anthracene structure changes so little and so smoothly between 295 K and 94 K (see Figs. 6 and 7) that any such phase transition would have to be very subtle.

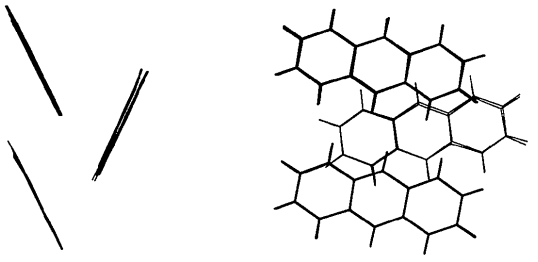

Fig. 6. Two views of the anthracene structure; each view shows the superposition of the structures determined at 295 and 94 K. In both drawings the **b** axis points upwards. In the view on the left the normal to the molecular plane in the lower left is in the plane of the drawing; rotation from this view by 90° around **b** gives the view on the right. The overlap of the bottom pair of molecules has been maximized. (This figure was produced by the program *MOMO* written at the ETH, Zurich, by Professor M. Dobler.)

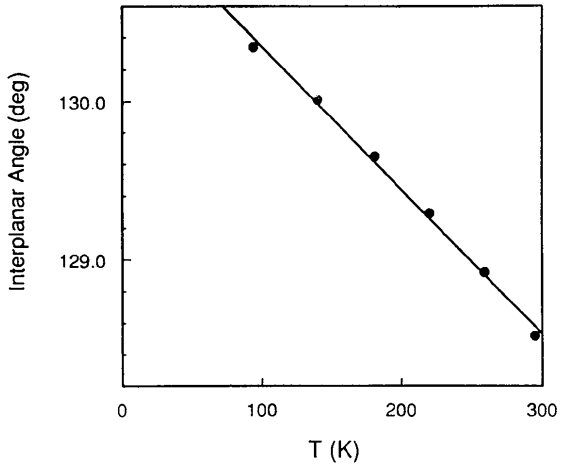

Fig. 7. Change with temperature of the angle between the C-atom planes of two anthracene molecules related by a 2_1 axis or an *a* glide plane. The root-mean-square deviation of the six points from the least-squares line is 0·03°.

Concluding remarks

It will be necessary to carry out additional work in order to determine whether or not the anomalous temperature dependence of the **L** tensor is real. The size of the change in the $L^{11}_{\rm int}$ value relative to its e.s.d. must be raised. One approach would be to repeat the study for several more crystals. Another would be to improve the quality of the desciption of the thermal motion by replacing the spherical atomic scattering factors with multipole expansions. Efforts in the latter direction will be described in a subsequent paper (Brock, Dunitz & Hirshfeld, 1991).

We are indebted to Professor Sven Cyvin for carrying out the calculations of the amplitudes of the internal motions, to Paul Seiler for his assistance during data collection, to Bernd Schweizer for his help with many aspects of the calculations, and to Professor Fred Hirshfeld for helpful discussions and penetrating insights.

References

ADAMS, D. M. & TAN, T.-K. (1981). *J. Chem. Soc. Faraday Trans.* 2, **77**, 1711–1714.

ALLEN, F. H., BELLARD, S., BRICE, M. D., CARTWRIGHT, B. A., DOUBLEDAY, A., HIGGS, H., HUMMELINK, T., HUMMELINK-PETERS, B. G., KENNARD, O., MOTHERWELL, W. D. S., RODGERS, J. R. & WATSON, D. G. (1979). *Acta Cryst.* B**35**, 2331–2339.

BAKKE, A., CYVIN, B. N., WHITMER, J. C., CYVIN, S. J., GUSTAVSEN, J. E. & KLAEBOE, P. (1979). *Z. Naturforsch. Teil A*, **34**, 579–584.

BROCK, C. P. & DUNITZ, J. D. (1982). *Acta Cryst.* B**38**, 2218–2228.

BROCK, C. P., DUNITZ, J. D. & HIRSHFELD, F. L. (1991). *Acta Cryst.* B**47**. Submitted.

BROCK, C. P. & WEBSTER, D. F. (1976). *Acta Cryst.* B**32**, 2089–2094.

CHAPLOT, S. L., LEHNER, N. & PAWLEY, G. S. (1982). *Acta Cryst.* B**38**, 483–487.

CRAIG, D. P., OGILVIE, J. F. & REYNOLDS, P. A. (1976). *J. Chem. Soc. Faraday Trans.* 2, **72**, 1603–1612.

CRIADO, A. (1989). *Acta Cryst.* A**45**, 409–415.

CROMER, D. T. & WABER, J. T. (1974). *International Tables for X-ray Crystallography*, Vol. IV, Tables 2.2B and 2.3.1. Birmingham: Kynoch Press. (Present distributor Kluwer Academic Pubishers, Dordrecht.)

CRUICKSHANK, D. W. J. (1956*a*). *Acta Cryst.* **9**, 915–923.

CRUICKSHANK, D. W. J. (1956*b*). *Acta Cryst.* **9**, 1005–1009.

CRUICKSHANK, D. W. J. (1957). *Acta Cryst.* **10**, 470.

CRUICKSHANK, D. W. J. & SPARKS, R. A. (1960). *Proc. R. Soc. London Ser. A*, **258**, 270–285.

CYVIN, S. J. (1981). Personal communication.

CYVIN, S. J., CYVIN, B. N., HAGEN, G., CRUICKSHANK, D. W. J. & PAWLEY, G. S. (1972). *Molecular Structures and Vibrations*, edited by S. J. CYVIN, pp. 299–309. Amsterdam: Elsevier.

DORNER, B., BOKHENKOV, E. L., CHAPLOT, S. L., KALUS, J., NATKANIEC, I., PAWLEY, G. S., SCHMELZER, U. & SHEKA, E. F. (1982). *J. Phys. C*, **15**, 2353–2365.

DUNITZ, J. D., SCHOMAKER, V. & TRUEBLOOD, K. N. (1988). *J. Phys. Chem.* **92**, 856–867.

DUNITZ, J. D. & SEILER, P. (1973). *Acta Cryst.* B**29**, 589–595.

FILIPPINI, G., GRAMACCIOLI, C. M., SIMONETTA, M. & SUFFRITTI, G. B. (1973). *J. Chem. Phys.* **59**, 5088–5101.
FILIPPINI, G., GRAMACCIOLI, C. M., SIMONETTA, M. & SUFFRITTI, G. B. (1974). *Acta Cryst.* A**30**, 189–196.
GOURSOT, P., GIRDHAR, H. L. & WESTRUM, E. F. (1968). *C. R. Acad. Sci. Ser. C*, **266**, 949–950.
GRAMACCIOLI, C. M., FILIPPINI, G., SIMONETTA, M., RAMDAS, S., PARKINSON, G. M. & THOMAS, J. M. (1980). *J. Chem. Soc. Faraday Trans.* 2, **76**, 1336–1346.
HIRSHFELD, F. L., HOPE, H. & RABINOVICH, D. (1990). In preparation.
JANKOWIAK, R., BÄSSLER, H. & KUTOGLU, A. (1985). *J. Phys. Chem.* **89**, 5705–5709.
JINDAL, V. K., KALUS, J., BOKHENDOV, E. L., CHAPLOT, S. L., DORNER, B., NATKANIEC, I., PAWLEY, G. S. & SHEKA, E. F. (1982). *J. Phys. C*, 7283–7294.
LEHMANN, M. S. & PAWLEY, G. S. (1972). *Acta Chem. Scand.* **26**, 1996–2004.
MASON, R. (1964). *Acta Cryst.* **17**, 547–555.
MATHIESON, A. MCL., ROBERTSON, J. M. & SINCLAIR, V. C. (1950). *Acta Cryst.* **3**, 245–250.
MIRSKY, K. & COHEN, M. (1978). *Chem. Phys. Lett.* **54**, 40–41.
NEERLAND, G., CYVIN, B. N., BRUNVOLL, J., CYVIN, S. J. & KLAEBOE, P. (1980). *Z. Naturforsch Teil A*, **35**, 1390–1394.
NICOL, M., VERNON, M. & WOO, J. T. (1975). *J. Chem. Phys.* **63**, 1992–1999.
PARKINSON, G. M., GORINGE, M. J., RAMDAS, S., WILLIAMS, J. O. & THOMAS, J. M. (1978). *J. Chem. Soc. Chem. Commun.* pp. 134–135.
PAULING, L. (1960). *The Nature of the Chemical Bond*, 3rd ed. Ithaca: Cornell Univ. Press.
PAULING, L. (1980). *Acta Cryst.* B**36**, 1898–1901.
PAWLEY, G. S. (1967). *Phys. Status Solidi*, **20**, 347–360.
PONOMAREV, V. I. & SHILOV, G. V. (1983). *Sov. Phys. Crystallogr.* **28**, 397–399.
PUFALL, R. & KALUS, J. (1988). *Acta Cryst.* A**44**, 1059–1065.
RAMDAS, S., PARKINSON, G. M., THOMAS, J. M., GRAMACCIOLI, C. M., FILIPPINI, G., SIMONETTA, M. & GORINGE, M. J. (1980). *Nature (London)*, **284**, 153–154.
ROBERTSON, J. M. (1933). *Proc. R. Soc. London Ser. A*, **140**, 79–98.
ROSENFIELD, R. E. JR, TRUEBLOOD, K. N. & DUNITZ, J. D. (1978). *Acta Cryst.* A**34**, 828–829.
ROSS, R. G., ANDERSSON, P. & BÄCKSTRÖM, G. (1979). *Mol. Phys.* **38**, 527–533.
RYZHENKOV, A. I., KOZHIN, V. M. & MYASNIKOVA, R. M. (1969). *Sov. Phys. Crystallogr.* **13**, 896–898.
SEILER, P., SCHWEIZER, W. B. & DUNITZ, J. D. (1984). *Acta Cryst.* B**40**, 319–327.
SINCLAIR, V. C., ROBERTSON, J. M. & MATHIESON, A. MCL. (1950). *Acta Cryst.* **3**, 251–256.
SPARKS, R. A. (1958). PhD Thesis, Univ. of California.
STEWART, J. M., KRUGER, G. J., AMMON, H. L., DICKINSON, C. & HALL, S. R. (1972). The *XRAY*72 system – version of June 1972. Tech. Rep. TR-192. Computer Science Center, Univ. of Maryland, College Park, Maryland, USA.
SUZUKI, M., YOKOYAMA, T. & ITO, M. (1968). *Spectrochim. Acta*, **24A**, 1091–1107.
TRUEBLOOD, K. N. (1978). *Acta Cryst.* A**34**, 950–954.
VOVELLE, F., CHEDIN, M.-P. & DUMAS, G. G. (1978). *Mol. Cryst. Liq. Cryst.* **48**, 261–271.

Acta Cryst. (1990). B**46**, 806–823

Structure Determination of Quinoprotein Methylamine Dehydrogenase from *Thiobacillus versutus*

BY F. M. D. VELLIEUX, K. H. KALK, J. DRENTH AND W. G. J. HOL

BIOSON Research Institute, Department of Chemistry, University of Groningen, Nijenborgh 16, 9747 *AG Groningen, The Netherlands*

(*Received* 2 *March* 1990; *accepted* 31 *May* 1990)

Abstract

The crystal structure of quinoprotein methylamine dehydrogenase from *Thiobacillus versutus* (EC 1.4.99.3, $M_r = 123\,500$) has been solved to 2·25 Å resolution. The crystals of space group $P3_121$ ($a = b = 129{\cdot}8$, $c = 104{\cdot}3$ Å) contain half a tetrameric enzyme molecule in the asymmetric unit, with a solvent content of *ca* 70%. The procedure used to solve this structure involved multiple isomorphous-replacement phasing, complemented by phase extension using solvent flattening, and phase combination with partial-model phases. The use of solvent flattening was essential to generate good quality electron density maps into which initial models were built. These partial models were refined using molecular-dynamics procedures. Refined model phases were then combined with solvent-flattening phases to generate improved electron density distributions. In the absence of an amino-acid sequence for this enzyme, the current 2·25 Å resolution electron density map was interpreted to provide a model for the complete molecule. The crystallographic *R* factor for this model, which lacks any water molecules, is 28·6% for data between 6·0 and 2·25 Å resolution.

Introduction

Bacterial methylamine dehydrogenase (abbreviated as MADH, EC 1.4.99.3) is a periplasmic enzyme which contains a pyrroloquinoline quinone (PQQ)

0108-7681/90/060806-18$03.00